bioRxiv preprint doi: https://doi.org/10.1101/2022.06.29.497979; this version posted July 4, 2022. The copyright holder for this preprint (which was not certified by peer review) is the author/funder, who has granted bioRxiv a license to display the preprint in perpetuity. It is made available under aCC-BY 4.0 International license.

The role of proton in a eukaryotic zinc transporter

Senfeng Zhang[1‡], Chunting Fu[1‡], Yongbo Luo[2‡], Qingrong Xie[1], Tong Xu[1], Ziyi Sun[1]*, Zhaoming Su[2]*, Xiaoming Zhou[1]*

[1]Department of Integrated Traditional Chinese and Western Medicine, Rare Diseases Center, State Key Laboratory of Biotherapy, West China Hospital, Sichuan University, Chengdu, Sichuan 610041, China

[2]The State Key Laboratory of Biotherapy, Department of Geriatrics and National Clinical Research Center for Geriatrics, West China Hospital, Sichuan University, Chengdu, Sichuan 610041, China

[‡]These authors contributed equally to this work.

*To whom correspondence should be addressed:

Ziyi Sun, PhD, 17 Renmin Road South 3rd Section, Sichuan University, Chengdu, Sichuan 610041, China; Phone: +86 (28) 8540 1152; Email: ziyi.sun@scu.edu.cn

Zhaoming Su, PhD, 17 Renmin Road South 3rd Section, Sichuan University, Chengdu, Sichuan 610041, China; Phone: +86 (28) 8540 5028; Email: zsu@scu.edu.cn

Xiaoming Zhou, PhD, 17 Renmin Road South 3rd Section, Sichuan University, Chengdu, Sichuan 610041, China; Phone: +86 (28) 8540 1152; Email: x.zhou@scu.edu.cn

Running head:

The role of H^+ in ZnT8

bioRxiv preprint doi: https://doi.org/10.1101/2022.06.29.497979; this version posted July 4, 2022. The copyright holder for this preprint (which was not certified by peer review) is the author/funder, who has granted bioRxiv a license to display the preprint in perpetuity. It is made available under aCC-BY 4.0 International license.

Abstract

Zinc transporter 8 (ZnT8) is mainly expressed in pancreatic islet β cells and is responsible for H^+-coupled uptake (antiport) of Zn^{2+} into insulin secretory granules. Structures of human ZnT8 and its prokaryotic homolog YiiP have provided structural basis for constructing a plausible transport cycle for Zn^{2+}. However, the mechanistic role that H^+ plays in the transport process remains elusive. Here we present two cryo-EM structures of ZnT8 from *Xenopus tropicalis* (xtZnT8) captured in the presence of either abundant Zn^{2+} or abundant H^+. Combined with a microscale thermophoresis analysis, our data suggest that binding of Zn^{2+} to the transmembrane Zn^{2+}-binding site drives xtZnT8 to the outward-facing state. Surprisingly, binding of H^+ to xtZnT8 is not sufficient to drive the transporter to an inward-facing state, suggesting that protonation alone is not a determining factor to establish an inward-facing conformation during Zn^{2+} transport. Instead, the role of protonation appears to unbind and release Zn^{2+} from the transmembrane site in the outward-facing state of xtZnT8, thus allowing an inward-facing isomerization to occur for the next cycle.

bioRxiv preprint doi: https://doi.org/10.1101/2022.06.29.497979; this version posted July 4, 2022. The copyright holder for this preprint (which was not certified by peer review) is the author/funder, who has granted bioRxiv a license to display the preprint in perpetuity. It is made available under aCC-BY 4.0 International license.

Introduction

Zinc is the second most abundant trace metal in cells and plays critical roles in many biological processes, including cell growth and development, functioning of the central nervous system and the immune system[1-3]. A variety of enzymes also require Zn^{2+} for their biological functions[1-3]. Meanwhile, excessive cytoplasmic free Zn^{2+} is highly toxic. Therefore, the intracellular homeostasis of Zn^{2+} is tightly controlled, mainly by two classes of solute carrier (SLC) transporters: the ZRT/IRT-like proteins (ZIPs, or SLC39), and the cation-diffusion facilitators (CDFs, or SLC30), also known as zinc transporters (ZnTs)[3-5]. These two transporter families mediate influx and efflux of Zn^{2+} into and out of the cytoplasm of the cell, respectively. Among ZnTs, ZnT8 is mainly expressed in pancreatic islet β cells and is responsible for H^+-coupled uptake/antiport of Zn^{2+} into insulin secretory granules, in which Zn^{2+} is complexed with insulin in a crystalline form and is co-secreted with insulin[6]. ZnT8 is often targeted by autoantibodies in type 1 diabetes[7,8], whereas mutations and single nucleotide polymorphisms of ZnT8 are associated with type 2 diabetes[9-13].

High-resolution structures of the ZnT family were first obtained with its prokaryotic homolog, YiiP from *Escherichia coli* (ecYiiP)[14,15] or *Shewanella oneidensis* (soYiiP)[16-18], revealing a homodimeric configuration of YiiP. The former was captured in an outward-facing conformation while the latter in an inward-facing conformation, based on which an alternating-access model was proposed for Zn^{2+} transport in YiiP[17,19-21]. Recently, structures of human ZnT8 (hZnT8) were determined by single-particle electron cryomicroscopy (cryo-EM)[22], also as a homodimer (Fig. 1A). Four Zn^{2+}-binding sites were identified in each hZnT8 protomer: one S_{TMD} site at the center of the transmembrane domain (TMD), two adjacent S_{CTD} sites in the carboxy-terminal domain (CTD), and one $S_{interface}$ site at the interface between TMD and CTD (Fig. 1A). S_{TMD} is the primary site for Zn^{2+} binding and transport, whereas the S_{CTD} sites are formed by residues from both protomers and contribute to hZnT8 dimerization and stability. These three Zn^{2+}-binding sites are highly conserved in the ZnT family (Supplementary Fig. 1), including the prokaryotic YiiP. On the other hand, the $S_{interface}$ site is much less conserved. In hZnT8, it is formed by residues from both CTD and a loop region between TM2 and TM3[22], while in YiiP it is formed solely by residues from the TM2-TM3 loop[14,17]. In some species like mouse and rat, no Zn^{2+}-coordinating residue (Cys, His, Glu or Asp) is present within the predicted TM2-TM3 loop (Supplementary Fig. 1), further indicating that $S_{interface}$ may not be conserved. Nonetheless, it has been hypothesized that $S_{interface}$ may increase the local concentration of Zn^{2+} to facilitate its binding to the S_{TMD} site in ZnT8[22].

The hZnT8 structures were captured in both outward-facing and inward-facing states, allowing construction of a Zn^{2+} transport cycle for eukaryotic ZnT8 transporters[22]. In both conformations, the two S_{CTD} sites of each hZnT8 protomer are occupied by two Zn^{2+} with little conformational change, indicating that the S_{CTD} Zn^{2+} do not participate directly in the transport cycle. Therefore, a simplified alternating-access model proposed previously could well explain the transport function for ZnT8 in the following steps[22] (Fig. 1B). (1) Due to the slightly basic cytosolic pH[23,24], a counter-transported H^+ is released to the cytosol from ZnT8 in the inward-open state, allowing a cytosolic Zn^{2+} to bind to the S_{TMD} site. (2) Zn^{2+} binding drives ZnT8 to the outward-facing state (i.e. the inward-to-outward-facing transition). (3) The S_{TMD}-bound Zn^{2+} is released to

bioRxiv preprint doi: https://doi.org/10.1101/2022.06.29.497979; this version posted July 4, 2022. The copyright holder for this preprint (which was not certified by peer review) is the author/funder, who has granted bioRxiv a license to display the preprint in perpetuity. It is made available under aCC-BY 4.0 International license.

the granule lumen while the acidic luminal pH[25] protonates the S_{TMD} site of ZnT8. (4) ZnT8 transits back to the inward-facing state (i.e. the outward-to-inward-facing transition), ready for the next cycle. The model is consistent with the structural and functional data reported for ZnTs regarding H^+-coupled Zn^{2+} binding and transport[22,26,27]. However, mechanistic details of the H^+ function in this process remain elusive.

In this study, we report two cryo-EM structures of ZnT8 from *Xenopus tropicalis* (xtZnT8) captured in the presence of abundant Zn^{2+} or abundant H^+. Together with a microscale thermophoresis analysis that monitors conformational changes of xtZnT8, our findings help to elucidate the role of protonation during Zn^{2+} transport in ZnT8.

Results

Cryo-EM structure of xtZnT8 with Zn^{2+} in an outward-facing state

Based on this model, Zn^{2+} and H^+ appear to be the two driving factors for directional conformational changes in the transport cycle of ZnT8 (Fig. 1B, step 2 and step 4, respectively). Herein, we determined two structures of xtZnT8 in the presence of either abundant Zn^{2+} (1 mM Zn^{2+}, 3.85 Å, termed xtZnT8-Zn^{2+}) (Supplementary Fig. 2) or abundant H^+ (pH 5.5, 3.72 Å, termed xtZnT8-H^+) (Supplementary Fig. 3) by cryo-EM, to analyze the Zn^{2+}/H^+-driven conformations. XtZnT8 shares 58% sequence identity and 83% sequence similarity to hZnT8 (Supplementary Fig. 1), and it is also organized as a homodimer similarly to hZnT8 and YiiP.

In the presence of Zn^{2+}, xtZnT8-Zn^{2+} resembles closely the hZnT8-Zn^{2+} structure (PDB: 6XPE) and adopts an outward-facing conformation in both protomers (Fig. 2A). Structural alignment between individual protomers from xtZnT8-Zn^{2+} and hZnT8-Zn^{2+} yielded an RMSD of 1.18 Å with all C_{α} atoms aligned, while the major deviation came from relatively flexible loop regions of the two proteins. Similar to hZnT8-Zn^{2+}, xtZnT8-Zn^{2+} has one Zn^{2+} bound at the S_{TMD} site with a tetrahedral coordination, which is formed by His100 and Asp104 from TM2, and His225 and Asp229 from TM5 (Fig. 2B and Supplementary Fig. 1). The S_{TMD} residues are highly conserved in eukaryotic species with the 2-His-2-Asp configuration, whereas prokaryotic YiiP proteins have a slightly different 1-His-3-Asp configuration[21,28]. Like the hZnT8-Zn^{2+} structure, the S_{TMD}-bound Zn^{2+} in xtZnT8-Zn^{2+} is accessible by solvent from the luminal side (Fig. 2C), indicating that the transporter is in an outward-open state. This result is consistent with the notion that Zn^{2+} binding at S_{TMD} drives ZnT8 to the outward-facing conformation (Fig. 1B, step 2), which is also observed in YiiP[19]. Interestingly, this S_{TMD}-bound Zn^{2+} was not released automatically from the S_{TMD} site in the outward-open state, suggesting that a Zn^{2+}-releasing mechanism is required for eukaryotic ZnT8. Similar to hZnT8-Zn^{2+}, each protomer of xtZnT8-Zn^{2+} has two adjacent S_{CTD} sites (S_{CTD1} and S_{CTD2}), which are formed by the HCH (His45-Cys46-His47) motif from one protomer and multiple Zn^{2+}-coordinating residues from the other protomer, occupied by two Zn^{2+} (Supplementary Fig. 1 and 4A).

Meanwhile, two major differences were observed between the xtZnT8-Zn^{2+} and hZnT8-Zn^{2+} structures. First, the region between the HCH motif and TM1 (termed HCH-TM1-linker) assumed an α helical structure as a continuation of the TM1 helix in xtZnT8-Zn^{2+}. In hZnT8-Zn^{2+}, HCH-TM1-linker was not resolved (Supplementary Fig. 4B), suggesting that this region may

bioRxiv preprint doi: https://doi.org/10.1101/2022.06.29.497979; this version posted July 4, 2022. The copyright holder for this preprint (which was not certified by peer review) is the author/funder, who has granted bioRxiv a license to display the preprint in perpetuity. It is made available under aCC-BY 4.0 International license.

adopt a flexible/unordered conformation, which may be involved in the outward-to-inward-facing transition (see the Discussion section). Second, even in the presence of 1 mM Zn^{2+}, no Zn^{2+} density was observed for the $S_{interface}$ site in xtZnT8-Zn^{2+} (His131/His350) (Supplementary Fig. 4C), which corresponds to His137/His345 in hZnT8 (Supplementary Fig. 1). This result suggests that the function of $S_{interface}$ is less conserved.

Cryo-EM structure of xtZnT8 at a low pH still in an outward-facing state

Then, we analyzed the structure of xtZnT8-H^{+} at pH 5.5, which is close to the internal pH of insulin secretory granules (5~6)[25]. It is tempting to postulate that binding of H^{+} to S_{TMD} of ZnT8 would drive the transporter to the inward-facing state (Fig. 1B, step 4), which serves as a H^{+}-coupling mechanism for Zn^{2+} antiport. However, intriguingly, the xtZnT8-H^{+} structure also adopts an outward-facing conformation, similar to xtZnT8-Zn^{2+} (Fig. 2D). This data suggests that protonation alone of xtZnT8 is not sufficient to drive the transporter to the inward-facing conformation.

Superposition of the two xtZnT8 structures yielded an all-atom RMSD of 0.58 Å, indicating that xtZnT8-H^{+} and xtZnT8-Zn^{2+} are very alike (Fig. 2D). The most prominent difference between the two structures is that the side chain of His100 in xtZnT8-H^{+} is pointing toward the luminal side, thus disrupting the tetrahedral coordination for Zn^{2+} at the S_{TMD} site (Fig. 2E). Two histidines of S_{TMD} (His100 and His225) are likely protonated at pH 5.5, which would cause disruption of Zn^{2+} coordination. Therefore, protonation of xtZnT8 in the outward-facing state likely causes unbinding and release of Zn^{2+} from S_{TMD}, as proposed previously for hZnT8[22] and YiiP[17,19]. Consistently, no Zn^{2+} density was observed at S_{TMD} in xtZnT8-H^{+} (Fig. 2F). Another difference between the two xtZnT8 structures is that a portion of TM2 (Ala93-Ala98), which is close to the luminal side, appears more flexible in xtZnT8-Zn^{2+} than in xtZnT8-H^{+}, and therefore is less visible in the former map (Supplementary Fig. 4D). This is reminiscent of hZnT8-Zn^{2+} (PDB: 6XPE) and the structure of its S_{TMD} double-mutant (hZnT8$_{D110N/D224N}$, PDB: 6XPD), which mimics a protonated state at the positions 110 and 224, and doesn't bind Zn^{2+} at the mutated S_{TMD} site[22]. Compared to hZnT8$_{D110N/D224N}$, the hZnT8-Zn^{2+} structure also shows a less defined TM2 portion near the luminal side (Supplementary Fig. 4E). These results suggest that Zn^{2+} binding at S_{TMD} increases the flexibility of this near-lumen TM2 region, whereas H^{+} binding at S_{TMD} stabilizes this region. Different conformations of the near-lumen TM2 region may play a role in regulating accessibility and binding of Zn^{2+}/H^{+} to the S_{TMD} site in ZnT8.

Conformational changes of xtZnT8 during Zn^{2+}/H^{+} binding

We then used the microscale thermophoresis (MST) technique to probe conformational changes of xtZnT8 during Zn^{2+}/H^{+} binding. MST measures the thermophoretic mobility of a protein in solution, which is mainly affected by its shape and size[29], and so the conformational information of the protein may be inferred. First, we tested the effect of Zn^{2+} binding to a wild-type xtZnT8 sample, which has been purified in the absence of Zn^{2+} at a physiological pH of 7.5. MST analysis showed that the plot of normalized fluorescent signals against Zn^{2+} concentrations readily fit an inverse S-shaped curve (Fig. 2G), with a higher level of fluorescent signals at lower

bioRxiv preprint doi: https://doi.org/10.1101/2022.06.29.497979; this version posted July 4, 2022. The copyright holder for this preprint (which was not certified by peer review) is the author/funder, who has granted bioRxiv a license to display the preprint in perpetuity. It is made available under aCC-BY 4.0 International license.

Zn^{2+} concentrations and a lower level of fluorescence at higher Zn^{2+} concentrations. The equilibrium dissociation constant (K_d) for Zn^{2+} is 4.91 ± 0.39 μM, slightly larger than previously reported affinity of S_{TMD} for Zn^{2+} in YiiP[14,28]. This data indicates that xtZnT8 transits from a lower thermophoretic mobility state (termed "low-mobility" state) to a higher thermophoretic mobility state (termed "high-mobility" state) upon Zn^{2+} binding (Fig. 2G), which likely corresponds to the xtZnT8-Zn^{2+} structure (outward-facing state) (Fig. 2A). Therefore, it is reasonable to postulate that the "low-mobility" state may correspond to an inward-facing-like state.

Then we monitored conformational changes of purified xtZnT8 during H^+ binding in the absence of Zn^{2+}. Surprisingly, titrating xtZnT8 with H^+ also yielded an inverse S-shaped MST curve similar to the Zn^{2+} titration (Fig. 2H), suggesting that protonation of xtZnT8 also transits the transporter from the "low-mobility" state (inward-facing-like) to a "high-mobility" state (outward-facing), which is consistent with the xtZnT8-H^+ structure (Fig. 2D). The equilibrium dissociation constant (K_d) for H^+ is 0.28 ± 0.02 μM, which corresponds to ~pH 6.55, close to the pK_a of histidine side chain (~6.0). This data further indicates that H^+ binding to xtZnT8 is less likely a driving factor for the inward-facing conformation.

Discussion

In this study, we provide insight into the driving force of ZnT8 to its inward-facing state (Fig. 1B, step 4). From a thermodynamic perspective, the outward-to-inward-facing transition of ZnT8 is achieved either by an external driving factor with energy input, or by an internal thermodynamic equilibrium of conformational isomerization. Apparently, counter-transport of H^+ along its electrochemical gradient would be a tempting driving factor to couple to the antiport of Zn^{2+} in ZnT8. However, our cryo-EM structure of xtZnT8-H^+ (Fig. 2D) and its thermophoretic mobility analysis (Fig. 2H) refute protonation as the determining factor that drives the outward-to-inward-facing transition in ZnT8. Therefore, our data would favor the second possibility that the inward-facing conformation could be achieved by thermodynamic conformational equilibrium of ZnT8. Meanwhile, our data also show that Zn^{2+} binding to S_{TMD} drives xtZnT8 to the outward-facing state (Fig. 2A and 2G). So, protonation of the S_{TMD} site to disrupt Zn^{2+} coordination and to release Zn^{2+} would be a prerequisite for the inward isomerization of ZnT8. This hypothesis is consistent with a heterogeneous conformation observed for hZnT8 captured in the absence of Zn^{2+} (PDB: 6XPF), which contains one protomer in the outward-facing conformation while the other in the inward-facing conformation with no Zn^{2+} in the S_{TMD} site[22].

Furthermore, a particularly intriguing region of eukaryotic ZnT8 proteins is the HCH motif and HCH-TM1-linker. The HCH motif participates directly in the formation of the S_{CTD} sites and remains mostly unchanged during the Zn^{2+} transport cycle[22]. However, TM1 moves substantially during the outward-to-inward-facing transition of ZnT8. For example, Glu66 near the amino-end of TM1 in hZnT8 moves > 10 Å away from the dimer center during the outward-to-inward-facing transition (PDB: 6XPF, protomer B to A) (Supplementary Fig. 4F). The nearly fixed HCH motif and the highly mobile TM1 indicate that HCH-TM1-linker has to unwind from an α helical structure (outward-facing state) to an unordered loop structure (inward-facing state), to

bioRxiv preprint doi: https://doi.org/10.1101/2022.06.29.497979; this version posted July 4, 2022. The copyright holder for this preprint (which was not certified by peer review) is the author/funder, who has granted bioRxiv a license to display the preprint in perpetuity. It is made available under aCC-BY 4.0 International license.

accommodate the increased distance between the HCH motif and the TM1 helix (Supplementary Fig. 4F). Consistently, HCH-TM1-linker was not resolved in the hZnT8 structures (Supplementary Fig. 4B), suggesting that this region may adopt a flexible/unordered conformation. It is noteworthy that prokaryotic YiiP proteins have no HCH motif, and their S_{CTD} sites do not involve any residues before the TM1 helix[14,17]. Therefore, compared to prokaryotic YiiP proteins, eukaryotic ZnT8 proteins have one more structural coupling (i.e. HCH-to-TM1) between the CTD and TMD regions, which may provide additional mechanism for regulating conformational changes as previously suggested[22].

References

1. Vallee, B.L. & Falchuk, K.H. The biochemical basis of zinc physiology. *Physiol Rev* **73**, 79-118 (1993).
2. Maret, W. Zinc biochemistry: from a single zinc enzyme to a key element of life. *Adv Nutr* **4**, 82-91 (2013).
3. Kambe, T., Tsuji, T., Hashimoto, A. & Itsumura, N. The Physiological, Biochemical, and Molecular Roles of Zinc Transporters in Zinc Homeostasis and Metabolism. *Physiol Rev* **95**, 749-84 (2015).
4. Bin, B.H., Seo, J. & Kim, S.T. Function, Structure, and Transport Aspects of ZIP and ZnT Zinc Transporters in Immune Cells. *J Immunol Res* **2018**, 9365747 (2018).
5. Eide, D.J. Zinc transporters and the cellular trafficking of zinc. *Biochim Biophys Acta* **1763**, 711-22 (2006).
6. Davidson, H.W., Wenzlau, J.M. & O'Brien, R.M. Zinc transporter 8 (ZnT8) and beta cell function. *Trends Endocrinol Metab* **25**, 415-24 (2014).
7. Wenzlau, J.M. et al. The cation efflux transporter ZnT8 (Slc30A8) is a major autoantigen in human type 1 diabetes. *Proc Natl Acad Sci U S A* **104**, 17040-5 (2007).
8. Kawasaki, E. ZnT8 and type 1 diabetes. *Endocr J* **59**, 531-7 (2012).
9. Sladek, R. et al. A genome-wide association study identifies novel risk loci for type 2 diabetes. *Nature* **445**, 881-5 (2007).
10. Scott, L.J. et al. A genome-wide association study of type 2 diabetes in Finns detects multiple susceptibility variants. *Science* **316**, 1341-5 (2007).
11. Flannick, J. et al. Loss-of-function mutations in SLC30A8 protect against type 2 diabetes. *Nat Genet* **46**, 357-63 (2014).
12. Saxena, R. et al. Genome-wide association analysis identifies loci for type 2 diabetes and triglyceride levels. *Science* **316**, 1331-6 (2007).
13. Zeggini, E. et al. Replication of genome-wide association signals in UK samples reveals risk loci for type 2 diabetes. *Science* **316**, 1336-41 (2007).
14. Lu, M. & Fu, D. Structure of the zinc transporter YiiP. *Science* **317**, 1746-8 (2007).
15. Lu, M., Chai, J. & Fu, D. Structural basis for autoregulation of the zinc transporter YiiP. *Nat Struct Mol Biol* **16**, 1063-7 (2009).
16. Coudray, N. et al. Inward-facing conformation of the zinc transporter YiiP revealed by cryoelectron microscopy. *Proc Natl Acad Sci U S A* **110**, 2140-5 (2013).

bioRxiv preprint doi: https://doi.org/10.1101/2022.06.29.497979; this version posted July 4, 2022. The copyright holder for this preprint (which was not certified by peer review) is the author/funder, who has granted bioRxiv a license to display the preprint in perpetuity. It is made available under aCC-BY 4.0 International license.

17. Lopez-Redondo, M.L., Coudray, N., Zhang, Z., Alexopoulos, J. & Stokes, D.L. Structural basis for the alternating access mechanism of the cation diffusion facilitator YiiP. *Proc Natl Acad Sci U S A* **115**, 3042-3047 (2018).
18. Lopez-Redondo, M. et al. Zinc binding alters the conformational dynamics and drives the transport cycle of the cation diffusion facilitator YiiP. *J Gen Physiol* **153**(2021).
19. Gupta, S. et al. Visualizing the kinetic power stroke that drives proton-coupled zinc(II) transport. *Nature* **512**, 101-4 (2014).
20. Sharma, G. & Merz, K.M. Mechanism of Zinc Transport through the Zinc Transporter YiiP. *J Chem Theory Comput* **18**, 2556-2568 (2022).
21. Cotrim, C.A., Jarrott, R.J., Martin, J.L. & Drew, D. A structural overview of the zinc transporters in the cation diffusion facilitator family. *Acta Crystallogr D Struct Biol* **75**, 357-367 (2019).
22. Xue, J., Xie, T., Zeng, W., Jiang, Y. & Bai, X.C. Cryo-EM structures of human ZnT8 in both outward- and inward-facing conformations. *Elife* **9**(2020).
23. Llopis, J., McCaffery, J.M., Miyawaki, A., Farquhar, M.G. & Tsien, R.Y. Measurement of cytosolic, mitochondrial, and Golgi pH in single living cells with green fluorescent proteins. *Proc Natl Acad Sci U S A* **95**, 6803-8 (1998).
24. Stiernet, P., Nenquin, M., Moulin, P., Jonas, J.C. & Henquin, J.C. Glucose-induced cytosolic pH changes in beta-cells and insulin secretion are not causally related: studies in islets lacking the Na+/H+ exchangeR NHE1. *J Biol Chem* **282**, 24538-46 (2007).
25. Hutton, J.C. The internal pH and membrane potential of the insulin-secretory granule. *Biochem J* **204**, 171-8 (1982).
26. Shusterman, E. et al. ZnT-1 extrudes zinc from mammalian cells functioning as a Zn(2+)/H(+) exchanger. *Metallomics* **6**, 1656-63 (2014).
27. Ohana, E. et al. Identification of the Zn2+ binding site and mode of operation of a mammalian Zn2+ transporter. *J Biol Chem* **284**, 17677-86 (2009).
28. Hoch, E. et al. Histidine pairing at the metal transport site of mammalian ZnT transporters controls Zn2+ over Cd2+ selectivity. *Proc Natl Acad Sci U S A* **109**, 7202-7 (2012).
29. Jerabek-Willemsen, M., Wienken, C.J., Braun, D., Baaske, P. & Duhr, S. Molecular interaction studies using microscale thermophoresis. *Assay Drug Dev Technol* **9**, 342-53 (2011).

bioRxiv preprint doi: https://doi.org/10.1101/2022.06.29.497979; this version posted July 4, 2022. The copyright holder for this preprint (which was not certified by peer review) is the author/funder, who has granted bioRxiv a license to display the preprint in perpetuity. It is made available under aCC-BY 4.0 International license.

Data Availability

The cryo-EM density maps for xtZnT8-Zn^{2+} and xtZnT8-H^+ have been deposited in the Electron Microscopy Data Bank under the accession IDs EMD-33619 and EMD-33620, respectively. The atomic coordinates of the xtZnT8-Zn^{2+} and xtZnT8-H^+ structures have been deposited in the Protein Data Bank under the accession codes 7Y5G and 7Y5H, respectively. Three previously published hZnT8 structures and one soYiiP structure used in this study are available in the Protein Data Bank under accession codes 6XPD, 6XPE, 6XPF and 5VRF. Source data of K_d values are provided with this paper.

Acknowledgements and Funding

Cryo-EM data were collected at SKLB West China Cryo-EM Center and were processed at the Duyu High Performance Computing Center of Sichuan University. This work was supported in part by the National Natural Science Foundation of China (NSFC) grant 31770783 to Xiaoming Zhou and 32070049 to Zhaoming Su, the 1.3.5 Project for Disciplines of Excellence grant by West China Hospital of Sichuan University to Xiaoming Zhou and Zhaoming Su, and Ministry of Science and Technology of China grant 2021YFA1301900 to Zhaoming Su.

Author Contributions

Senfeng Zhang, Functional study, Cryo-EM sample preparation, Data analysis; Chunting Fu, Functional study, Cryo-EM data processing, Data analysis; Yongbo Luo, Cryo-EM data collection, Data analysis; Qingrong Xie, Functional study, Data analysis; Tong Xu, Functional study; Ziyi Sun, Conceptualization, Supervision, Data analysis; Zhaoming Su, Supervision, Data analysis; Xiaoming Zhou, Conceptualization, Supervision, Cryo-EM model building and validation, Data analysis. Ziyi Sun and Xiaoming Zhou wrote the manuscript with input from all authors.

Competing Interests

The authors declare no competing financial interests.

bioRxiv preprint doi: https://doi.org/10.1101/2022.06.29.497979; this version posted July 4, 2022. The copyright holder for this preprint (which was not certified by peer review) is the author/funder, who has granted bioRxiv a license to display the preprint in perpetuity. It is made available under aCC-BY 4.0 International license.

Figure Legends

Figure 1. Structure and a working model for ZnT8. (A) Cryo-EM structure of hZnT8 in the presence of Zn^{2+} in an outward-facing conformation (PDB: 6XPE). The hZnT8 dimer is displayed in cartoon mode with two protomers colored in green and orange, respectively. Bound Zn^{2+} are rendered as red spheres in one protomer only for better viewing. Transmembrane segments of each protomer are numbered from one to six. The relative position of the granule membrane is indicated by two grey lines. (B) A simplified alternating-access model for ZnT8. The dimeric ZnT8 is displayed in surface mode with two protomers colored in green and orange, respectively. S_{TMD}-Bound H^{+}/Zn^{2+} are rendered as spheres as indicated. The outward-facing and inward-facing models were generated using the PDB structures 6XPE and 5VRF, respectively.

Figure 2. Structures of xtZnT8 in the outward-facing state. (A) Cryo-EM structure of xtZnT8 captured in the presence of 1 mM Zn^{2+} (xtZnT8-Zn^{2+}). The xtZnT8-Zn^{2+} dimer is displayed in orange, with one protomer in cartoon mode and the other as ribbons. Bound Zn^{2+} are shown as blue spheres. One protomer of the hZnT8-Zn^{2+} structure (PDB: 6XPE) is displayed in green with bound Zn^{2+} rendered as red spheres, and is superimposed onto xtZnT8-Zn^{2+}. The relative position of the granule membrane is indicated by two grey lines. (B) One Zn^{2+} (blue sphere) binds to the S_{TMD} site in xtZnT8-Zn^{2+}. The Zn^{2+}-coordinating residues are displayed as sticks. The cryo-EM map of xtZnT8-Zn^{2+} is shown as grey densities. (C) One protomer of xtZnT8-Zn^{2+} is displayed as ribbons, which is colored in rainbow spectrum with blue for the amino-terminus. Bound Zn^{2+} are shown as blue spheres. The solvent-accessible space is shown as a red surface. The relative position of the granule membrane is indicated by two grey lines. (D) Cryo-EM structure of xtZnT8 captured at pH 5.5 (xtZnT8-H^{+}). The xtZnT8-H^{+} dimer is displayed in green, with a red surface indicating the solvent-accessible space for one protomer. One protomer of the xtZnT8-Zn^{2+} structure is displayed in orange and is superimposed onto xtZnT8-H^{+}. Bound Zn^{2+} are shown as spheres. The relative position of the granule membrane is indicated by two grey lines. (E) Comparison of the S_{TMD} site between xtZnT8-H^{+} (in green) and xtZnT8-Zn^{2+} (in orange). One Zn^{2+} (orange sphere) binds to S_{TMD} in xtZnT8-Zn^{2+}. The Zn^{2+}-coordinating residues are rendered as sticks. (F) The cryo-EM density map for the S_{TMD} site in xtZnT8-H^{+}. The Zn^{2+}-coordinating residues are rendered as sticks. (G) A representative MST curve for xtZnT8 titrated with Zn^{2+}. (H) A representative MST curve for xtZnT8 titrated with H^{+}.

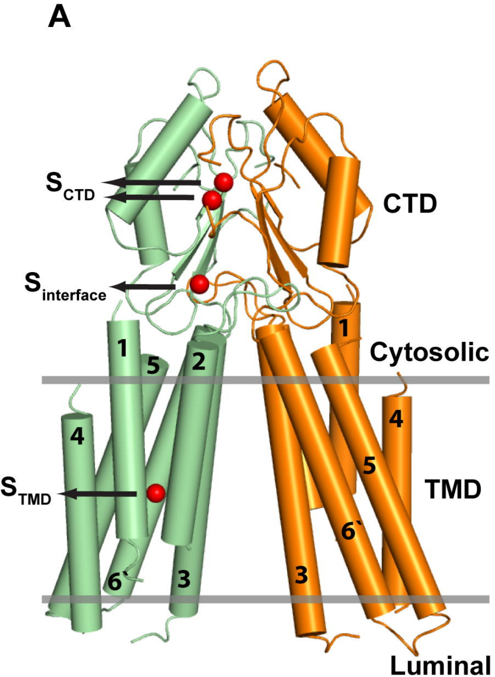

B

Cytosolic
pH 7.0-7.4
TMD
Luminal
H^+
Zn^{2+}
1
Inward-facing H^+-bound
Inward-facing Zn^{2+}-bound
4
Outward-to-inward
H^+ driving?
Inward-to-outward
Zn^{2+} driving?
2
3
Zn^{2+}
H^+
Cytosolic
Luminal
pH 5.0-6.0
Outward-facing H^+-bound
Outward-facing Zn^{2+}-bound

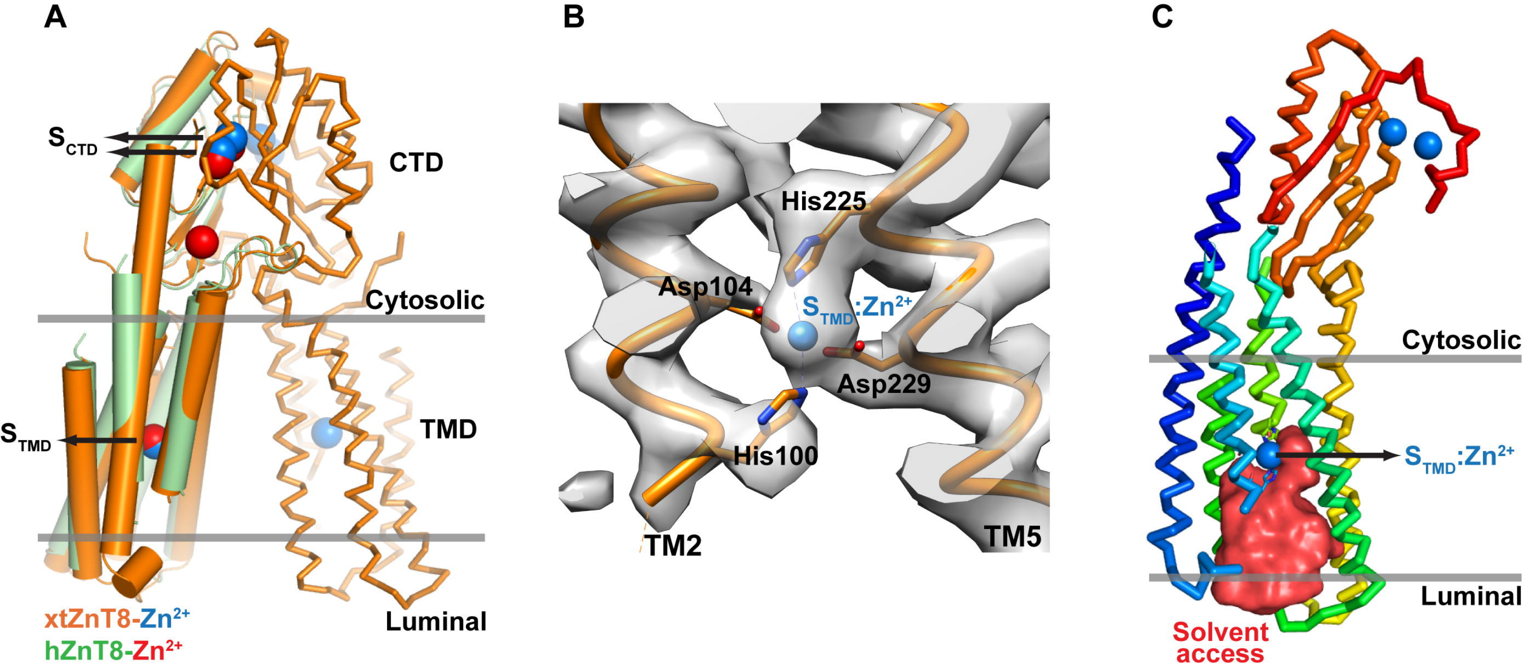
A
B
C
S_{CTD}
CTD
Cytosolic
S_{TMD}
TMD
Luminal
xtZnT8-Zn^{2+}
hZnT8-Zn^{2+}
His225
Asp104
S_{TMD}:Zn^{2+}
Asp229
His100
TM2
TM5
Cytosolic
S_{TMD}:Zn^{2+}
Luminal
Solvent access

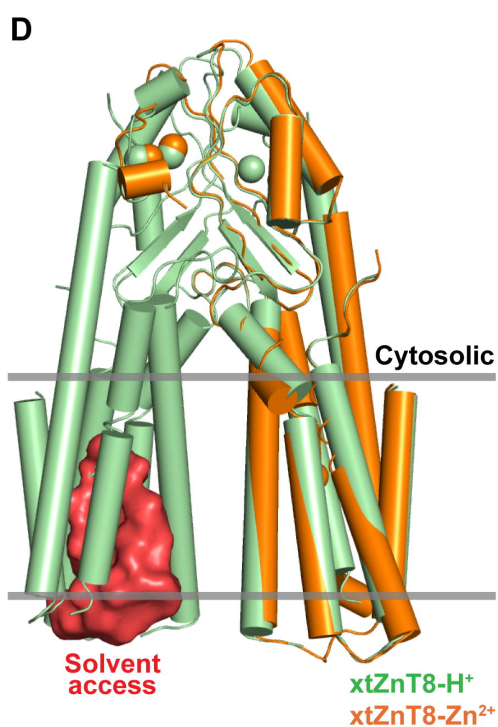
D
Cytosolic
Solvent access
xtZnT8-H^{+}
xtZnT8-Zn^{2+}

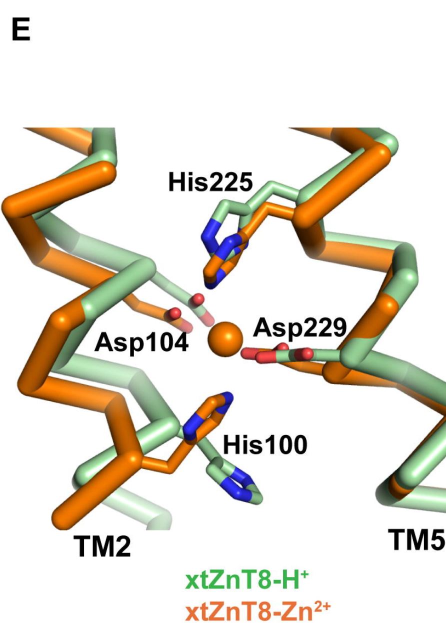
E
His225
Asp104
Asp229
His100
TM2
TM5
xtZnT8-H^{+}
xtZnT8-Zn^{2+}

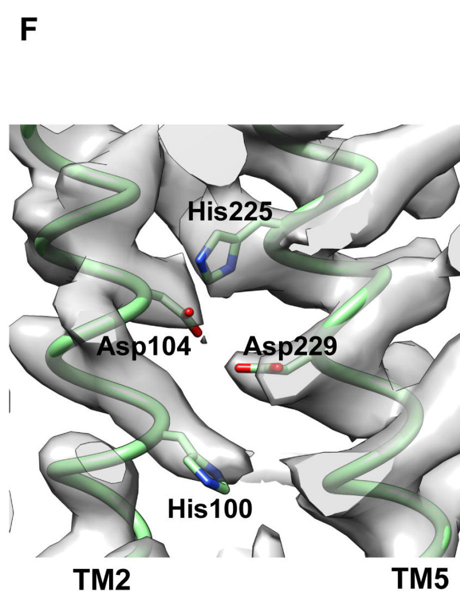
F
His225
Asp104
Asp229
His100
TM2
TM5

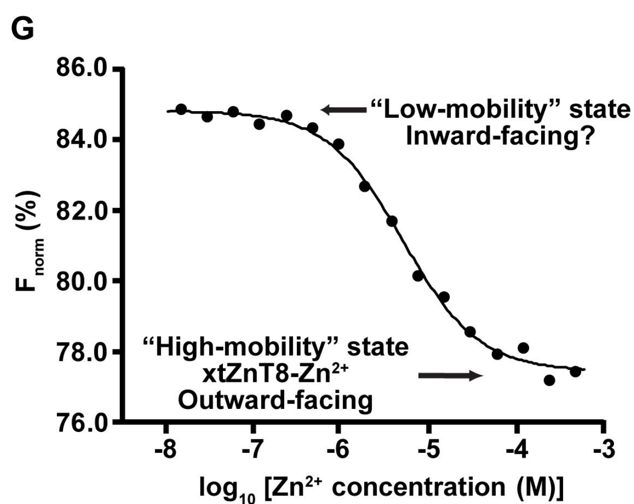
G
"Low-mobility" state
Inward-facing?
"High-mobility" state
xtZnT8-Zn^{2+}
Outward-facing
F_{norm} (%)
log_{10} [Zn^{2+} concentration (M)]

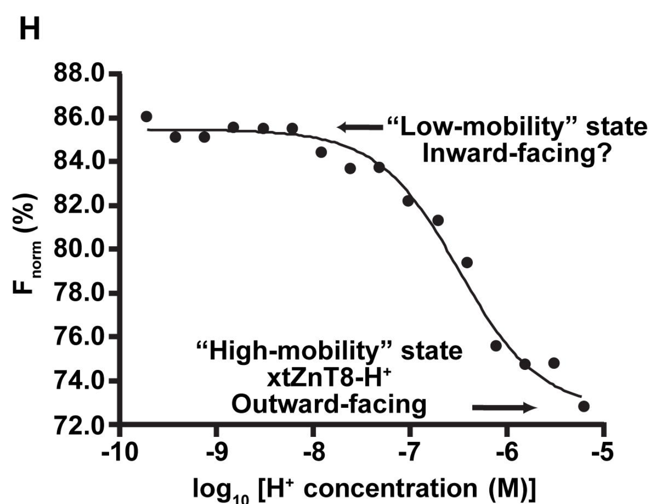
H
"Low-mobility" state
Inward-facing?
"High-mobility" state
xtZnT8-H^{+}
Outward-facing
F_{norm} (%)
log_{10} [H^{+} concentration (M)]